

Noise in Artificial Spin Ices

Anujan Ganeshalingam

Student Number: C1887983

Degree Programme: MPhys Physics

Supervisor: Dr. Felix Flicker

Primary Assessor: Dr. Sang Soon Oh

Secondary Assessor: Dr. Sam Ladak



School of Physics and Astronomy

Cardiff University

Year 4 Project Dissertation

Session 2021 - 2022

Declaration:

I have read and understand Appendix 2 in the Student Handbook: “Some advice on the avoidance of plagiarism”.

I hereby declare that the attached report is exclusively my own work, that no part of the work has previously been submitted for assessment (although it may re-use material from the “Summary Report” for **this project** as it is considered part of the same assessment), and that I have not knowingly allowed it to be copied by another person.

Noise in Artificial Spin Ices

Anujan Ganeshalingam

May 2022

School of Physics and Astronomy, Cardiff University

Word Count: 9426

Abstract

Spin ices are materials showcasing geometric frustration with degenerate states, within which emergent magnetic monopoles form. The characterisation of high frequency behaviour of the power spectral density is found through Monte Carlo simulations based on nearest neighbour and 16 vertex models for spin ices.

Two recent papers measuring the power spectral density are by *Kirschner et al.* [1] and *Samarakoon et al.* [2]. These both employ differing methods for the measurement of the magnetisation leading to very different forms of the power spectral density. In light of this, this project undertakes both methods independently to verify the decay exponent for the power spectral density and discuss which method is ultimately, correct.

Both methods are used to find the decay exponent of a 2D spin ice model using the nearest neighbour model between temperatures of $T \in [0.6, 1.1]$ K. The latter method is shown to oversample and identify the incorrect Nyquist frequency, leading to a power spectral density showing randomness rather than the characteristics of a spin ice with a decay exponent of $\beta \approx 1.95$ for the range of the temperatures. Whereas the former method identifies the correct power spectral density of the 2D spin ice model, finding decay exponents $\beta \approx 0.95$ for the range of temperatures. Correct decay exponents are also found from the *Samarakoon et al.* method through the correct identification of the Nyquist frequency, which agree with the results from the *Kirschner et al.* method, within errors of standard deviation.

Contents

1	Introduction	1
1.1	Artificial Spin Ice	1
1.2	Frustrated Systems	3
1.3	Nearest Neighbour Model	4
1.4	Dynamics	6
1.5	Power Spectral Density	7
1.6	Nyquist Frequency	10
2	Methodology	11
2.1	Monte Carlo Method	11
2.2	Dynamics of Nearest Neighbour Model	13
3	Results and Discussion	16
3.1	Dynamics of Nearest Neighbour Model	16
3.1.1	Measurement per Monte Carlo Step	16
3.1.2	Measurement per Attempted Spin	18
3.2	Future Work	22
4	Conclusion	23
5	Acknowledgements	26

1 Introduction

1.1 Artificial Spin Ice

Since the discovery of spin ices 25 years ago, research in this field has continued to grow tremendously. Spin ices include magnetic materials such as $\text{Dy}_2\text{Ti}_2\text{O}_7$ and $\text{Ho}_2\text{Ti}_2\text{O}_7$, where magnetic moments of particles, referred to as spins, live on the corners of pyrochlore (or tetrahedral) lattices, as seen in Figure 1 (a). These spins can point into or out of the lattice, where this direction can be flipped due to energetic excitations.

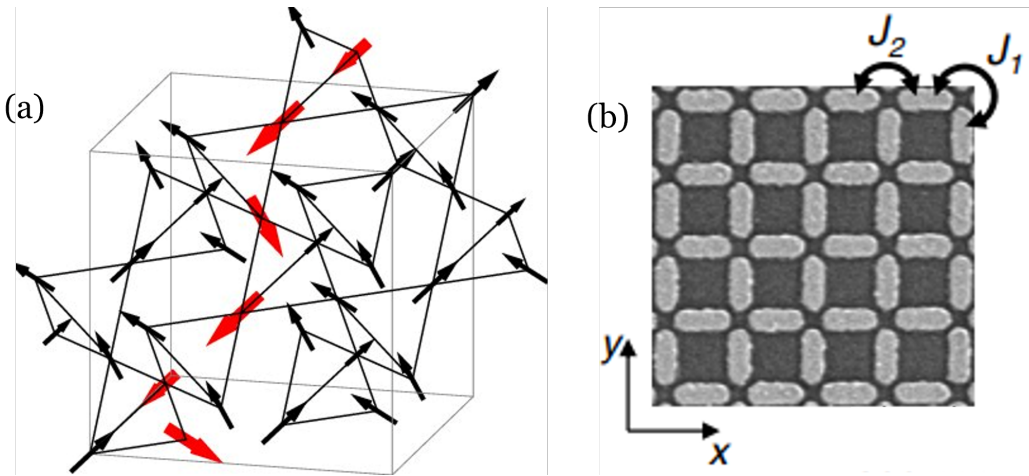


Figure 1: (a) shows an example of a 3D spin ice material with pyrochlore lattices with the spins pointing into and out of the lattice (figure from [3]) and (b) shows an image from a scanning electron microscope of an artificial 2D spin ice, showing the nearest neighbour coupling J_1 and next nearest neighbour coupling J_2 (figure from [4]).

Interestingly, these materials have degenerate energy states due to a concept named geometric frustration, whereby multiple configurations of the spins pointing in and out can have the same total energy. In fact, the name spin ice arises from Pauling's ice rules for water ice, which state that every atom of oxygen is connected to four other hydrogen atoms via bonds. Of these four bonds, two are strongly bonded and closer together, whilst the other two are weakly bonded and further away from the oxygen atom [5, 6]. This description of water ice was dubbed "two-near, two-far" by Pauling, causing degenerate

states in water ice since there were multiple options for the ground state. Similarly, in spin ices, the ground state is given by "two-in, two-out" spins in each tetrahedral vertex of the lattice. Further similarities include that both spin ice and water ice have the property of residual entropy at low temperatures. This is due to the degenerate ground state, since there are many variations for the system to take for the minimum energy configuration which fulfils the two-in, two-out rule; this randomness is represented as residual entropy [7].

In 2D, these spin ice materials can be artificially created using nanoscale magnets placed in a lattice formation, as shown in Figure 1 (b). These are created with the same geometric frustration from the two-in two-out rules and show similar types of properties to the 3D bulk materials. Similarly to the 3D materials where four spins sit on the corners of a tetrahedral lattice, for the 2D artificial spin ice, four spins sit on the square lattices in each vertex and can be conveniently described as 2×2 vertices. Advantageously, these 2D artificial spin ices can be made to measure, allowing for studies of the properties of the 3D bulk spin ices, such as specific phase transitions and frustration.

Another reason for the study of spin ices is due to the fact that they show emergent magnetic monopoles arising from excitations of the vertices. Initially hypothesised by *P. A. M. Dirac* [8], a magnetic monopole is an elementary particle with either only a north or a south pole, which is represented as magnetic charge. Whilst it has not been found as an independent particle, they are seen as emergent particles in spin ices, with these excitations causing areas of opposite magnetic charge, representing magnetic monopoles and antimonopoles. When a flipped spin causes the vertex to go from 2-in 2-out to 3-in (out) 1-out (in), magnetic monopoles are formed [9, 10], since locally there is an imbalance of net spin. The study of these emergent particles may even elucidate how to find magnetic monopoles as independent elementary particles, which is its own fundamental question.

We will focus on investigating the behaviour of the power spectral density of the 2D artificial spin ice model using Monte Carlo simulations. The power spectral density can be described as the noise power at different frequencies within the bandwidth and takes the form:

$$P(\omega) \propto \frac{1}{\omega^\beta} \quad (1)$$

where the power spectral density, $P(\omega)$ is proportional to the inverse of the frequency ω to some power β , known as the decay exponent [11].

1.2 Frustrated Systems

One of the main reasons for interest in spin ices is due to its geometric frustration. Frustration occurs when pairs of interactions cannot be satisfied simultaneously to produce a minimum energy configuration in a system [12]. In spin ices, the frustration occurs from the geometry. In the 3D case, vertices of four spins sit on a pyrochlore lattice with spins pointing in or out [13]. In the 2D case, the spins point in or out of 2×2 vertices in a square lattice. With the spins only being allowed to point in or out of the vertex, there are multiple arrangements to obtain a ground state, leading to geometric frustration.

The highly frustrated nature leads to multiple degenerate ground states, and in fact excited states as well, since the same overall energy is achieved through multiple configurations of the lattice for each state [14]. Specifically, the four spins from each 2×2 vertex can be represented as two sets of dipolar interactions and no configuration of the spins will connect such that the energy contributions from the dipole pairs are minimised [15].

In terms of the dipolar moments, two such moments are considered, which can be seen in Figure 1 (b). These are the nearest neighbour spin coupling J_1 , which is the closest nearby spin to each original spin and are perpendicular to each other in the vertex. The other is the next nearest neighbour spin coupling J_2 , which are co-linear and face opposite each other in the vertex. The resulting dipole energy of each set of moments are dependent on their alignment and maximised or minimised depending on the respective orientations of the spins. This means some vertices will naturally be more energetically favourable than others; the most favourable being when pairs of moment in each vertex point in the same direction [16]. Therefore, at lower temperatures, the spin ice will attempt to tend to these energetically favourable vertices for minimum

energy configurations. However, as discussed, the minimum energy state is degenerate, so there are many options for the spin ice to take.

1.3 Nearest Neighbour Model

The nearest neighbour model is based on the 2D artificial spin ice, where the spins are placed along the edges of the lattice, as seen in Figure 2. This placement of the spins means that directly perpendicular spins are nearest neighbour spins J_1 and co-linear spins are the next nearest neighbour spins J_2 as seen in 2D artificial spin ices in Figure 1 (b).

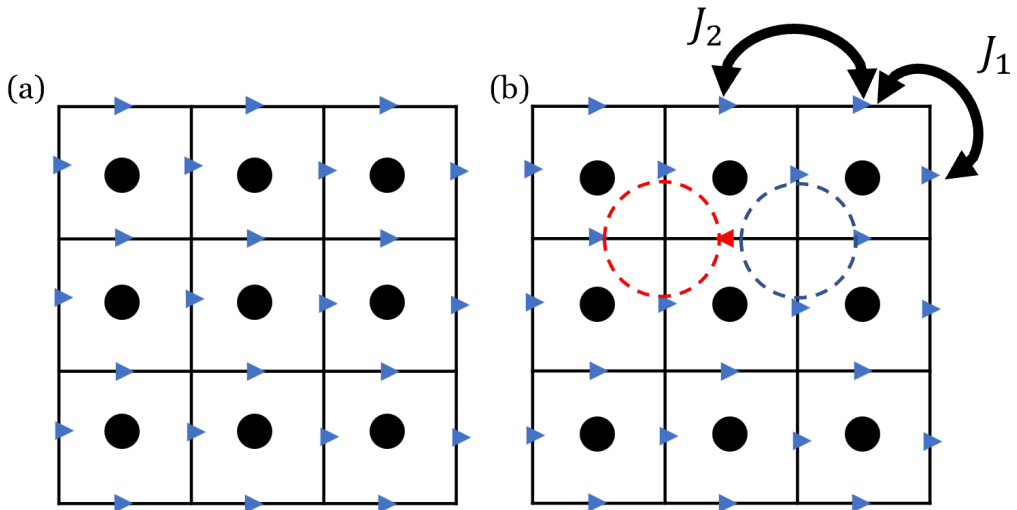


Figure 2: Nearest neighbour model emulates 2D artificial spin ices with spins of atoms on the edges of the lattice, where perpendicular spins are the nearest neighbour spins J_1 and co-linear spins are the next nearest neighbour spins J_2 , where (a) shows a completely ordered system at low temperatures, (b) shows a flipped spin due to thermal excitations, creating a monopole-antimonopole pair due to local differences in net spin density, represented by the red and blue circles.

These spins consequently point into or out of each vertex in the lattice, therefore also following the ice rules as seen in 3D spin ices and 2D artificial spin ices. For the ground state, a vertex of two-in two-out is required; Figure 2 (a) showing a system entirely at ground state.

As energy is increased in the system, excitations can occur, for example, the flipped spin seen in Figure 2 (b) causes areas which have greater or lesser

magnetic spin density than other nearby sites. Depending on the net spin of the region, these areas are interpreted as monopoles or antimonopoles, as seen in Figure 2 (b), by the red and blue circles respectively. Monopoles are defined to have a spin of $S = +1$, whereas antimonopoles are equal and opposite with spin $S = -1$.

This model is entirely comprised of four spins per vertex pointing in or out, meaning there are only a finite number of possibilities for the vertices. These options are represented by Figure 3, which is named the 16 vertex model [16]. This model collates vertex types with the same energies and net magnetisations with their corresponding probabilities of occurrence [17], denoted by a vertex type $a - e$. The ground state of 2-in 2-out is seen in vertex types a, b and c , each type varying in energy since the positions of the spins in the vertex define the energy [18]. This is since the nearest neighbour spins in alignment have a greater energy contribution than nearest neighbour spins which are not aligned, and similarly for the next nearest neighbour spins. Considering in and out spins to be equal and opposite, the net spin of the ground state is zero, since the spins cancel each other.

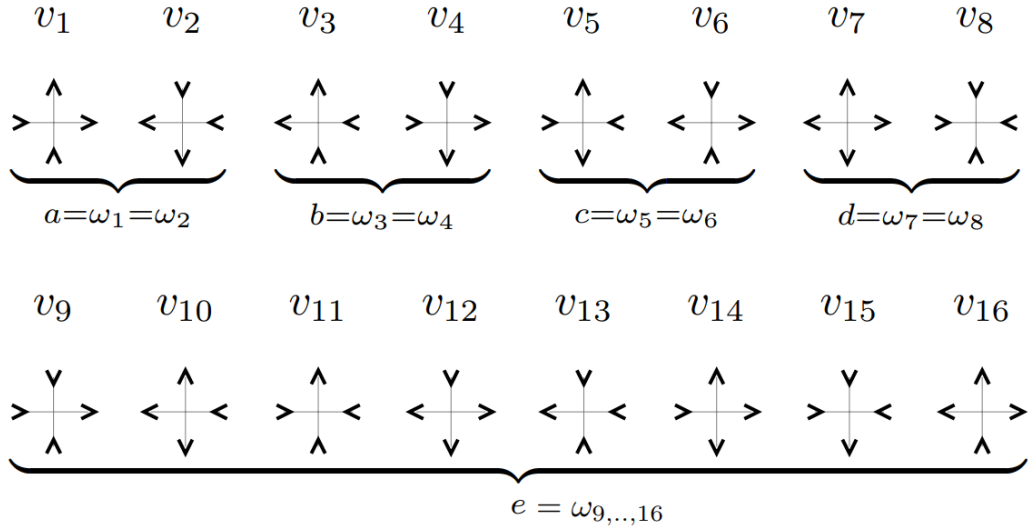


Figure 3: shows the 16 possible vertices for the nearest neighbour model, grouped into types $a - e$ by their net magnetisation, energies and resulting probabilities, figure from: [17].

Each of the vertex types, $a - e$ have a probability P , corresponding to the

form of $P = e^{\varepsilon_i/T}$, where ε_i is the energy of the vertex i [19].

1.4 Dynamics

In the monopole plasma regime of a spin ice, there are a large number of magnetic monopoles moving within the system. This can be achieved through an applied magnetic field \mathbf{B} , which is varied across the system. When a field is applied to the spins, they orient themselves along the field and therefore the energies of the system change. This means, the applied magnetic field can be enforced in the nearest neighbour model through changes of energy of the vertices, using energy distributions calculated by *M. Goryca et al.* [4], which represent the effect of applying a field onto the spin ice.

Here, the sixteen vertex model is used, whereby the energies of the vertices are defined by the nearest neighbour spin coupling J_1 measured between perpendicular spins and the next nearest neighbour spin coupling J_2 between co-linear spins, as seen in Figure 1 (b). It naturally follows that nearest neighbour spins in alignment have a greater energy contribution than next nearest neighbour spins in alignment, since there is a greater distance between the spins and the spins interact via a $1/r$ relationship [20], where r is the distance between the spins. The energies of each vertex is defined as:

$$\begin{aligned}\epsilon_a &= \epsilon_b = -2J_2, \\ \epsilon_c &= -4J_1 + 2J_2, \\ \epsilon_d &= 0, \\ \epsilon_e &= 4J_1 + 2J_2\end{aligned}\tag{2}$$

with the constraint that $J_1/J_2 = 1.8$ in the magnetic monopole plasma regime [4].

Using this, the temperature of the simulation is defined with units of J_2/k_b , where k_b is the Boltzmann's constant and easily controlled through the definitions of J_1 and J_2 .

For this system, the applied magnetic field is found using the energies of

the vertices and are controlled, once again, by the definitions of J_1 and J_2 as defined by:

$$|B_x| + |B_y| = \epsilon_a - \epsilon_c = 4(J_1 - J_2) \quad (3)$$

1.5 Power Spectral Density

Power spectral density is found through the Fourier transform of the auto-correlation function and is a common method to demonstrate the variation of time series data in terms of its corresponding frequency domain. It can be found for stochastic processes, such as Monte Carlo methods [21], representing how the data is spread across the frequency range of the measurements as it undergoes changes due to predefined variables for the setup.

Characterisation of the power spectral density is a very important concept for spin ices in general. At the temperatures used for 3D bulk spin ice materials such as $\text{Dy}_2\text{Ti}_2\text{O}_7$, whilst low, it still isn't low enough for the formation of single monopole excitations. When the spin ice is in the magnetic monopole plasma regime with a very high monopole density, there is a lot of movement, meaning any measurements of the magnetic flux or magnetisation becomes noisy. Due to this, taking the power spectral density of the noisy data allows for easier characterisation of the system, through the calculation of the decay exponent β , indicating the type of noise [22, 23].

Decay exponent of $\beta = 2$ is known as Brownian noise, since it represents a system with random processes, such as Brownian motion, the random movement of particles in a fluid. This decay exponent is also known as red noise due to the analogy with light. Since white light is a mixture of all frequencies, white noise is also defined as a mixture of all frequencies; red noise is comprised of more of the longer wavelengths, similarly to red light compared to white light. Whereas, a decay exponent of $\beta = 1$ is described to be pink noise and considering Eq. (1), this is known as $1/f$ noise. In 3D bulk materials, as magnetic flux is measured, the noise has been measured to go from white noise to pink noise [24], where white noise is given by $\beta = 0$.

An important condition to use power spectral density as a tool depends on whether the random processes are known as stationary process. This is when the probabilities of the system stay consistent through evolution of time of the measurement [25]. In the nearest neighbour model, the probabilities of the vertices are locked at the start of the simulations for each temperature corresponding to the energies of the vertices. Magnetisation is measured as a function of time for each temperature, allowing for the calculation of the power spectral density.

From literature, it is known that the power spectral density as a function of frequency $P(\omega)$ is given by the Fourier transform of $C(\tau)$, the autocorrelation function as a function of time [26], which measures the similarity between measurements of a time series. The autocorrelation function can be applied to the time series data produced by the measurements of magnetisation along Monte Carlo steps, represented by Eq. (4), between two successive temporal points in the magnetisation, where τ is an incremental time step.

The autocorrelation function measures the similarity of two sets of data with the same dimensions and number of data points between time lagged measurements [27, 28]. Autocorrelation values are normalised, therefore $C(\tau) = +1$ means a perfect positive correlation where all values in the dataset are identical, and $C(\tau) = -1$ means a perfect negative correlation where all values in the data have the opposite signs. High positive values for the autocorrelation function also indicates the influence of small changes over time and potential lack of long range ordering from the movement of monopoles. When the autocorrelation function tends to 0, this indicates no correlation between successive steps in the time series data, as expected from high temperatures in spin ice materials due to high rates of spin flips since there are increases in the energy of the system [29].

To find the power spectral density $P(\omega)$ of the magnetisation measurements, I performed the following derivation. The autocorrelation function $C(\tau)$ is first defined as the probability of finding the same magnetisation between two measurements with some time step τ :

$$C(\tau) = \langle M(t)M(t + \tau) \rangle \quad (4)$$

then, taking the Fourier transform from time to frequency space of Eq. (4) gives the integral:

$$\hat{C}(\omega) = \int_{-\infty}^{\infty} \langle M(t)M(t + \tau) \rangle e^{-i\omega\tau} d\tau \quad (5)$$

finding the autocorrelation function as a function of the frequency ω . The expectation value in Eq. (5) can be equally rewritten in the form of a double integral:

$$\hat{C}(\omega) = \frac{1}{L} \int_{-L/2}^{L/2} M(t) \int_{-\infty}^{\infty} M(t + \tau) e^{-i\omega\tau} d\tau dt \quad (6)$$

where L is the length of the lattice, therefore integrating over all the sites in the lattice. The variables t and τ are separated into the product of two integrals:

$$\hat{C}(\omega) = \frac{1}{L} \int_{-L/2}^{L/2} M(t) e^{i\omega t} dt \int_{-\infty}^{\infty} M(\tau') e^{-i\omega\tau'} d\tau' \quad (7)$$

which can be simplified to:

$$P(\omega) = \hat{C}(\omega) = \frac{1}{L} \left| \int_{-L/2}^{L/2} M(t) e^{-i\omega\tau} dt \right|^2 \quad (8)$$

under the limit of $L \rightarrow \infty$, Eq. (8) holds true and is in the form of a general power spectral density equation [30, 31], showing it can be calculated by taking the Fourier transform from time to frequency domain of the autocorrelated magnetisation. This derivation allows for easier calculation of the power spectral density through the autocorrelation and Fast Fourier Transform libraries. The power spectral density has the form given by Eq. (1), the decay constant β , being the focus of the noise characterisation of the nearest neighbour methods.

1.6 Nyquist Frequency

When taking Fourier transforms of discrete time series data, the issue of aliasing arises [32]. Aliasing occurs when the time series is undersampled when finding the Fourier transform, which causes a signal of a shorter period to appear as the signal of the real data which has a longer period. An example case is seen in Figure 4 showing some arbitrary test data. The real measured data is shown in blue, however measurements for the Fourier transform are taken over equal spacing greater than the period of the real data, leading to a perfectly viable interpolated wave shown in red, as a result of undersampling. Whilst it is indicative of the measured points, it does not convey the true nature of the data.

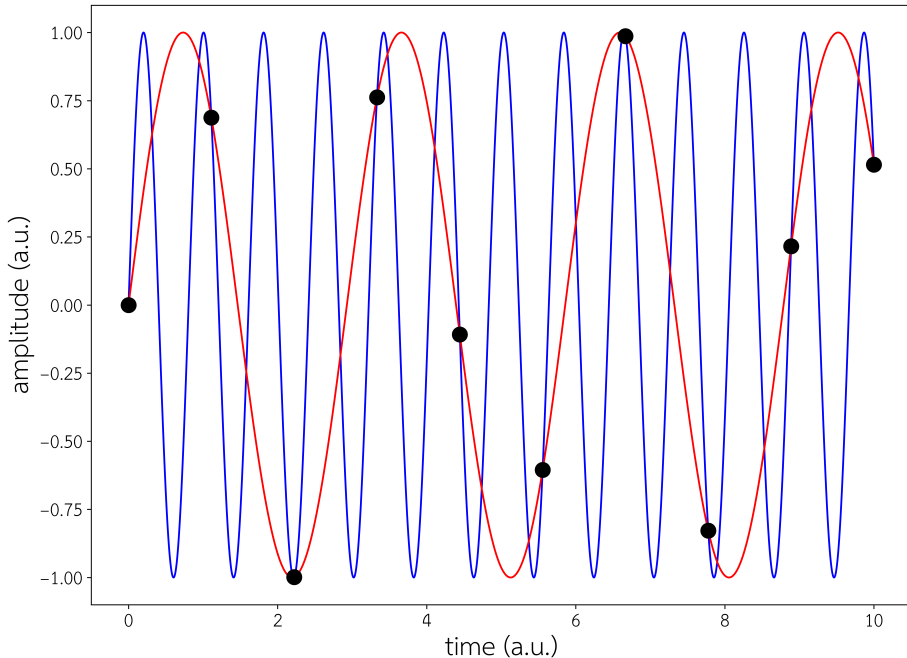


Figure 4: shows a case of undersampling; the blue sine wave is artificially created true data with a shorter period, with black dots representing equally spaced sampling points which are greater than the period of the true data and the resulting interpolated wave in red.

The aliasing is avoided by sampling faster than twice the Nyquist sampling rate, where the sampling rate is given by δT . In terms of the frequencies, which are reciprocal to their corresponding rates, this is shown by $f_s \geq 2f_c$ where f_s is the sampling frequency and f_c is the Nyquist frequency [33]. This is the minimum sampling speed needed to ensure the direction of changes of the data is recorded in the sampled values, meaning the most important part of the data is preserved through the signal processing.

The Nyquist frequency is therefore $f_c \leq f_s/2$, meaning the Nyquist frequency must be equal to half the sampling frequency or lower, therefore measurements should be recorded under this rate. When the Fourier transform of the time series data is taken in this report, this concept is applied to avoid aliasing.

Whilst aliasing occurs due to undersampling, oversampling causes other issues, whereby the data of interest becomes a very small minority of the entire dataset [34], this is due to sampling continuing to occur for much longer once the system being measured reaches its equilibrium. Since the large majority of the data then becomes irrelevant to the study, it makes little sense to sample too significantly past the Nyquist frequency.

2 Methodology

2.1 Monte Carlo Method

The nearest neighbour model is simulated through the Monte Carlo method [35], which is a computational method that can be used to numerically solve problems with set probabilities. It is especially helpful when systems become too complicated to easily solve analytically.

In a real spin ice, the size of the material is much greater than the lattice length, however such a large system is not feasible to be numerically modelled, since the number of sites would be of the order of $\sim 10^{23}$. For all simulations, periodic boundary conditions are applied so that smaller lattices can be used, assisting with the use of computational resources, whilst still emulating the

periodic nature of real bulk crystal spin ice materials. Periodic boundary conditions stipulate that each edge of the system links to its opposite edge.

To measure the dynamics of the nearest neighbour model, the Monte Carlo method was used for a variety of temperatures and therefore applied magnetic fields, meaning the energies are fixed for each applied field. To begin, an $L \times L$ lattice is created, where L is the length of the lattice, with a randomised spin of +1 or -1 placed on each site, representing in or out spins. This emulates a completely randomised spin ice material at high temperatures, since the high energy creates a random distribution of spins.

From this $L \times L$ lattice, the system is broken down into a set of 2×2 vertices to match and find their energies due to the 16 vertex model. From this, a random site is chosen to have its spin checked to see whether it should be flipped according to the following rules. These rules state that a spin is always allowed to be flipped if the energy change of the system from the flip is negative. If the energy change from the flip would be positive, the following condition is checked to see if the spin is flipped. The Boltzmann probability of the flip is calculated using

$$P = e^{\frac{-\Delta}{T}} \quad (9)$$

where Δ is the change in energy due to the flipped spin and T is the temperature of the system. If this probability is greater than a random number produced between 0 and 1, the flip is allowed to occur, emulating similar dynamics to spin ice materials as not all flips are always allowed whilst the system heads to energetically stable configurations.

When a spin is flipped in these systems, there is a change in energy corresponding to the vertices shown in the 16 vertex model in Figure 3 [36]. For example, taking a 2-in 2-out vertex and flipping the in spin to an out spin, produces a vertex with 1-in 3-out, and since the energies of each of the possible 16 vertices are known, the change in energy from this flip can be found. In addition, it should be noted, from Figure 2, flipping a single spin not only affects a single vertex, but the other neighbouring vertices too, therefore the change in energy of the entire surrounding set of vertices must be found.

This process is repeated N times per Monte Carlo step, where N is the total number of sites in the lattice. Each Monte Carlo step can be considered as a single time step. At each step, the magnetisation of the system is calculated using

$$M = \frac{\sum_{i,j} S_{i,j}}{N} \quad (10)$$

which is the sum of the total spins in the system, normalised by the number of the spins, therefore giving ± 1 for ordered systems with spins pointing in the same direction and 0 for disordered systems [37].

The magnetisation captured here is used to find the power spectral density, as covered in Section 1.5. Though the 2D case is considered due to ease of simulations, this application of the power spectral density is directly comparable to the bulk 3D spin ices, since in that case the magnetic flux is found and its power spectral density is found. This makes it important for the correct method of sampling to be identified. The whole Monte Carlo method is repeated 10^3 times and averaged for each applied magnetic field to reduce the noise of the power spectral density.

2.2 Dynamics of Nearest Neighbour Model

In terms of the dynamics of the nearest neighbour model, two different methods are applied for the measurement of the magnetisation of the system, to investigate a disparity in decay exponents within current literature.

The effects of the applied magnetic field are modelled through changes of the energy of the vertices. This naturally follows from real spin ice materials, since applying a magnetic field interacts with the spins within the vertices such that the total energy of the vertex is affected.

The applied magnetic field for the model is defined by

$$\mathbf{B} = \frac{4(J_1 - J_2)}{\mu} \quad (11)$$

through the difference between the couplings J_1 and J_2 and μ which is the

magnetic moment, taken to be 1 for this system.

The applied field is easily defined through the simulation temperature T of the system, which is represented by $T = J_2/k_b$, where k_b is the Boltzmann constant. The nearest neighbour constant and next nearest neighbour constant also have the relationship $J_1/J_2 = 1.8$ in this regime.

This allows Eq. (11) to be simply rearranged as $\mathbf{B} = 3.2T\mathbf{k}_b$. This definition allows for the degeneracy of vertex types a, b and c in the ground state and achieve the monopole plasma regime, which contain a high number of magnetic monopoles. This allows for the most diffusive state of monopoles, allowing for tunable studies of the dynamics of magnetic charge.

To reiterate, emergent magnetic monopoles arise in spin ices when there are excitations of the 2×2 vertices from the ground state, represented by vertices a, b and c in the 16 vertex model to the first excited states represented by vertex e . These excitations occur when spins are allowed to flip when the probability due to the energy cost is greater than a random probability.

The lattice is set up with 10×10 points with periodic boundary conditions to replicate periodic crystals. For the Monte Carlo method, 10^4 equilibration steps are used to ensure the system does indeed reach the correct simulation temperature, since it is initialised with randomised spins at its sites. Then, 10^4 Monte Carlo steps are taken to measure the magnetisation for each applied magnetic field.

Firstly, using the method laid out by *Kirschner et al.* [1], the magnetisation of the system is recorded once per Monte Carlo step. Therefore, there will generally be considerable variation between measurements, since a flip is attempted for the number of points in the system, giving 100 attempts per step in this setup.

Then this is compared to the method alluded to by *Samarakoon et al.* [2], whereby the magnetisation is calculated each time a spin is checked to be flipped, regardless of whether the flip is successful or not. This increases the number of recorded points of the magnetisation by a factor of N , where N is the number of spins in the lattice, by a factor of 100 in this case. The former method is comparable to a measurement per time step, whereas the

latter measures 100 times within a single time step, which we believe to be oversampling.

In fact, *Samarakoon et al.* proposed their method since they believe *Kirschner et al.* undersampled their measurements of once per time step. However, we predicted their method oversamples the measurements, leading to the portion of interest which actually characterises the material to become the minority class [38]. This simply means this class is much smaller than the rest of the data set, and the majority class of the data set does not represent the material, making the data valueless.

Therefore, both methods were attempted and evaluated. We predicted that measurements per time step would retrieve a decay exponent which is truly representative of the characteristics of the spin ice, whereas measurements per attempted flip would lead to oversampling and incorrect decay exponents from the majority class.

The power spectral density was found for both methods, from which the decay exponent β , of the system can be extracted from the form of Eq. (1). In a graph with logarithmic axes of the power spectral density $P(\omega)$ against the corresponding frequency ω the gradient is equal to the decay exponent, β . This is trivially seen from taking the log of both sides of Eq. 1

$$\ln P(\omega) = -\beta \ln \omega \quad (12)$$

where the decay exponent can be explained as representing how quickly the power spectral density decreases as the frequency is increased up to the Nyquist frequency.

In theory, since the method where the magnetisation is measured at each attempted flip measures at an integer multiple of the initial rate (since it now measures N times per Monte Carlo step), it naturally includes a measurement at each Monte Carlo step included within it. This can be achieved by only extracting every N^{th} value from the high rate method. By conducting separate experiments of measuring once per Monte Carlo step and once per attempted spin and then extracting every N^{th} spin to obtain measurements per Monte Carlo step, the decay exponents of both measurements per Monte Carlo step

should agree within an error, since these are measurements of the same system.

3 Results and Discussion

3.1 Dynamics of Nearest Neighbour Model

Using the method in section 2.2 for a nearest neighbour model of a spin ice with a varying applied magnetic field, the decay exponent was found using two different methods for the measurements of the magnetisation. Firstly, the decay exponent was independently calculated by taking measurements of the magnetisation once at each Monte Carlo step.

Secondly, with the same setup of the system, measurements were taken for each attempted flip in the system, which increases the number of measurement points for the system by a factor of N following the methods outlined in Section 2.2. From this second method, the regularly extracted decay exponent is shown to be incorrect when considering the Nyquist frequency to be midway of the dataset. Then, the correct value of the decay exponent is found through the identification of the true Nyquist frequency, which is the midway Nyquist frequency corrected by a factor of N to compensate for the increased rate of measurement.

3.1.1 Measurement per Monte Carlo Step

The system is ranged between temperatures of $T \in [0.6, 1.1]$ K for ideal comparison with results from *Samarakoon et al.* [2]. This temperature range corresponds to an applied magnetic field of $\mathbf{B} \in [1.92k_b, 3.52k_b]$. For each applied magnetic field, the power spectral density is found, with the Nyquist frequency identified to be halfway through the frequency range. A straight line of the form Eq. 12 is fitted to the data, ensuring this is before the Nyquist frequency.

The resulting graph is shown for a single temperature of $T = 0.6$ K and applied field $\mathbf{B} = 1.92k_b$ in Figure 5 yielding a decay exponent of $\beta = 0.950 \pm 0.017$, where the error is obtained from the standard deviation of the power

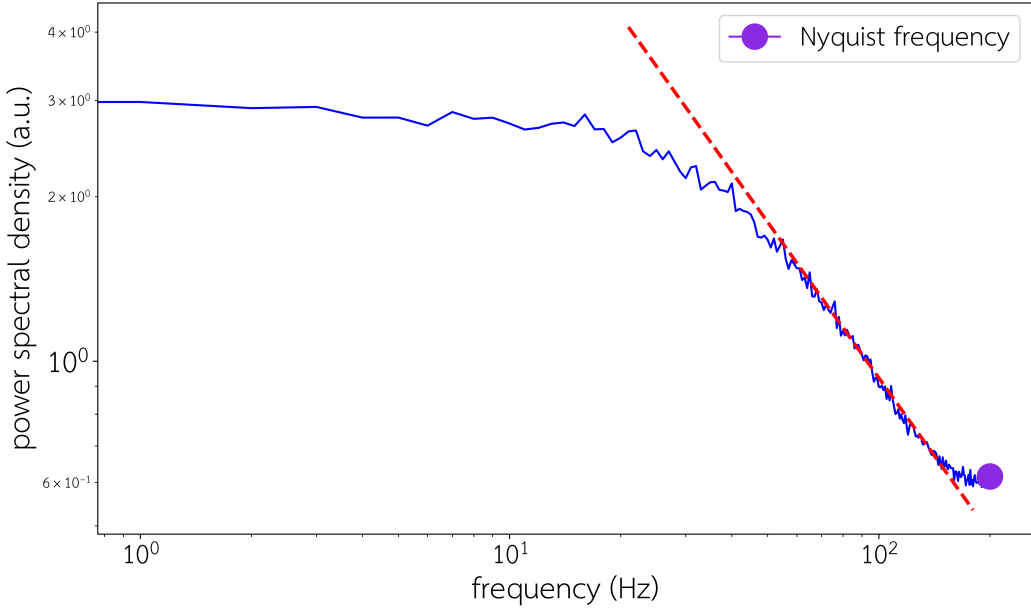


Figure 5: the power spectral density for an applied magnetic field $B = 1.92k_b$ or temperature $T = 0.6$ K as a function of frequency where measurements of magnetisation are recorded once per Monte Carlo step focusing on the frequency region up to the Nyquist frequency. The purple dot indicates the location of the Nyquist frequency, and the red dashed line shows the fitted straight line for the decay exponent for the given applied magnetic field. The graph is plotted on log axes, meaning the gradient of the fitted line gives the negative of the decay exponent, as per Eq. 12.

spectral density. The Nyquist frequency is indicated by the purple circle on the figure, therefore a straight line fit is applied to the straight line portion before the Nyquist frequency where the data begins to plateau and then reflects.

The decay exponents for the range of temperatures stay consistent within the error arising from the standard deviation of the sets of measurements, ranging between $\beta = 0.92$ and $\beta = 0.97$, indicating the applied magnetic field and simulation temperature have little to no impact on the decay exponent within this range. From the standard deviation calculations, the lowest value of the decay exponent is $\beta = 0.901$ for $T = 1.0K$ and the highest value is $\beta = 0.983$ for $T = 0.8K$.

3.1.2 Measurement per Attempted Spin

In this method, a measurement of the magnetisation is taken once per attempted flip for each Monte Carlo step. This is conducted over the same range as Section 3.1.1, with temperature $T \in [0.6, 1.1] K$ and corresponding applied field $\mathbf{B} \in [1.92k_b, 3.52k_b]$. Similarly again, the power spectral density is found for each applied magnetic field, as shown in Figure 6 for a single temperature of $T = 0.6K$ and applied magnetic field $\mathbf{B} = 1.92k_b$.

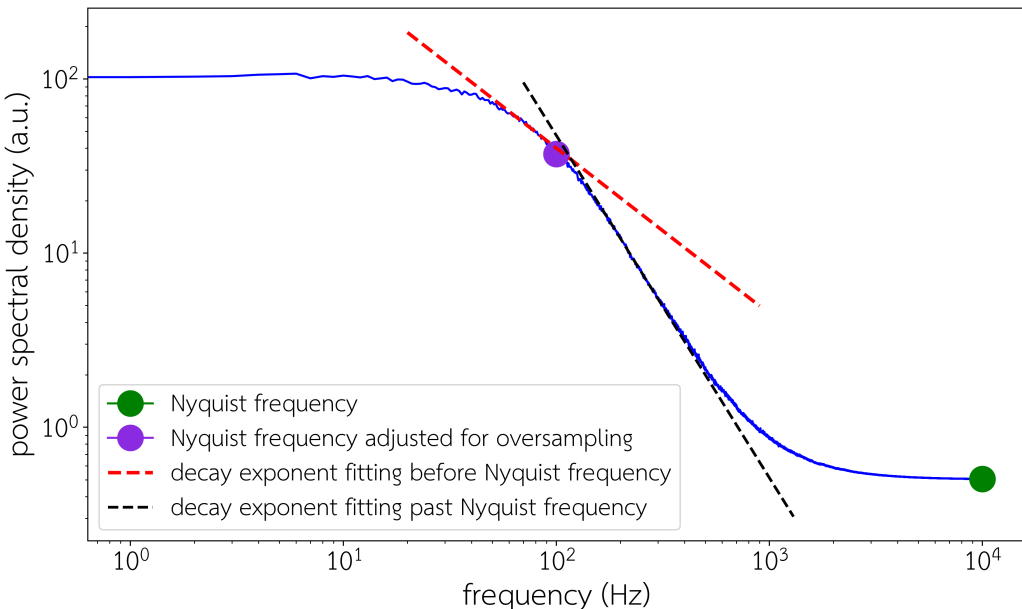


Figure 6: the power spectral density for applied magnetic field corresponding to $B = 1.92k_b$ or temperature $T = 0.6$ K as a function of frequency where measurements of magnetisation are recorded once each time a spin is attempted to be flipped in the Monte Carlo method, focusing on the frequency region up to and slightly greater than the Nyquist frequency. The purple dot indicating the location of the Nyquist frequency adjusted for oversampling, which will be referred to as the true Nyquist frequency. The red dashed line showing the fitted straight line before the true Nyquist frequency for the decay exponent for the given applied magnetic field and the black dashed line showing the fitting for frequencies greater than the true Nyquist frequency of the system tending to a gradient of 2. The green dot showing the position of the regular Nyquist frequency, also known as the folding frequency, at the middle frequency without compensating for increased sampling rate.

Previously, the Nyquist frequency was defined by its usual definition, which is simply the midpoint of the frequency range. This is sometimes also known

as the folding frequency, since it is where the data folds and is reflected [39]. However now, due to the increase in measurement points, the sampling rate is increased by the same factor and the Nyquist frequency isn't equal to the folding frequency. This means the position of the Nyquist frequency must be adjusted as well, reduced by a factor of N , due to the inverse relation between the sampling rate and Nyquist frequency. This adjusted Nyquist frequency is referred to as the true Nyquist frequency henceforth, and is represented by the purple dot in Figure 6, where the true Nyquist frequency is found by $f_c = f_s/2L^2$.

In Figure 6, two fitted lines are shown, the red dashed line shows the fit for the decay exponent for frequencies before the true Nyquist frequency, which we argue is in the correct position. The second line is the black dashed line, which is fit for the frequency range between the true Nyquist frequency and the second plateau. The red dashed line gives a decay exponent value of $\beta = 0.947 \pm 0.019$. From comparison to the decay exponent obtained from the independent method from Section 3.1.1 of $\beta = 0.950 \pm 0.017$, the values agree within their corresponding errors from the standard deviations at this temperature.

In fact, from Figure 7 it is seen that for each measured temperature, through comparison of the methods of independently measuring the magnetisation at each Monte Carlo step and extracting the decay exponent of measuring the magnetisation for each attempted spin from the placement of the correct Nyquist frequency, the decay exponents indeed do lie within their respective error bars. These errors are calculated from the standard deviation of the power spectral density of each temperature. The agreement between the two methods indicates the correct Nyquist frequency has been located in this method.

The method presented by *Samarakoon et al.* [2] shows the decay exponent tending to $\beta = 1.95$ for the exact same temperature range, also demonstrating that the decay exponent has no dependence on temperature in this regime. However, referring to Figure 6, the black dashed line shows a fit to the data for frequencies greater than the true Nyquist frequency, with a decay exponent

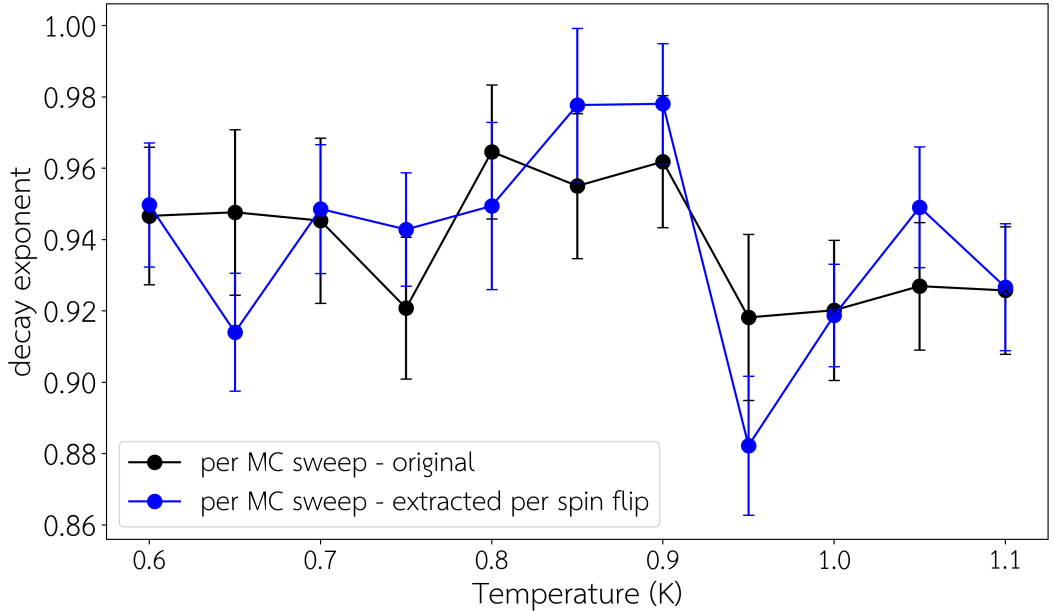


Figure 7: showing the decay exponents extracted for two sets of measurements as functions of the temperature; in black, the decay exponent for magnetisation measurements per Monte Carlo step. In blue, the decay exponent for magnetisation measurements per attempted spin flip, which has values taken every N^{th} value to extract the measurements which would be taken per Monte Carlo step.

of $\beta = 1.965 \pm 0.021$. The measured decay exponent from this region agrees with the values obtained by the *Samarakoon et al.* paper, indicating their results are also from the same frequency region, where frequencies are greater than the true Nyquist frequency.

For frequencies greater than the Nyquist frequency, the results lose meaning; due to the nature of the Fourier transform [40], the data reflects itself about a plateau with gradient 0 at the middle of the frequency range, known as the folding frequency. Therefore, measuring too close to this plateau at the folding frequency is also incorrect since the decay exponent becomes affected by something that is not characterising the material, but rather a mathematical part of finding the Fourier transform in this manner. Both Figure 5 and Figure 6 are cut off at their midpoint Nyquist frequency, since for higher frequencies than the middle frequency, a process called folding occurs where the frequencies greater than the Nyquist frequency are "folded" into the lower

frequencies and mirrored by aliasing [41].

Due to the oversampling leading to the increase in the number of measured magnetisation points to be by a factor of N , the Nyquist frequency is identified to be smaller by the same factor. This splits Figure 6 into exactly 2 sections, one fitted by the red dashed line, obtaining results in line with taking measurements once per Monte Carlo step, and the other fitted by the black dashed line which shows oversampling, resulting in decay exponents agreeing with *Samarakoon et al.* [2].

Further reasoning that the portion shown by the black dashed line in Figure 6 demonstrates oversampling is shown in Figure 8. Figure 8 (a) shows an unconstrained random walk in 2D for 10^5 steps, therefore similar to the simulation length of the Nearest Neighbour model used. The unconstrained random walk is said to be a Markovian system, meaning it is a completely random process where the probability of the processes do not change through evolution of the system. Figure 8 (b) shows the corresponding power spectral density for the random walk, with a straight line fitted before its Nyquist frequency, giving a decay exponent of $\beta = 1.997 \pm 0.012$. Within the errors, the decay exponent of a 2D unconstrained random walk agrees with the decay exponent obtained from the oversampled method.

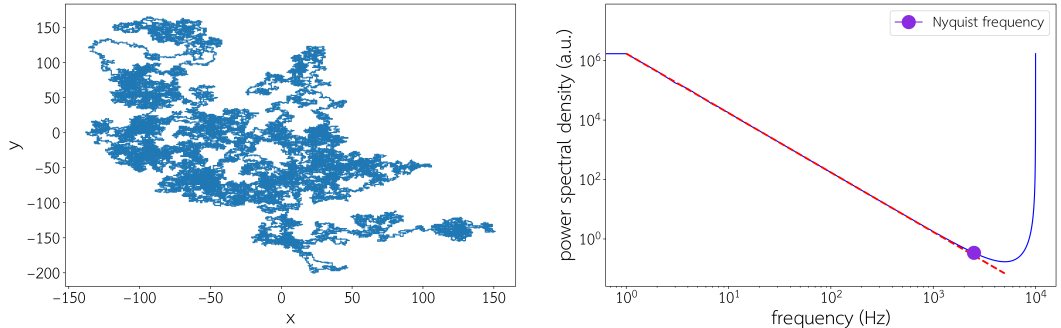


Figure 8: (a) shows an unconstrained 2D random walk for 10^5 steps and (b) shows its corresponding power spectral density, marked with the Nyquist frequency and a red dashed line to identify the decay exponent.

This can be explained by the fact that past the true Nyquist frequency in Figure 6, the high frequency regime directly corresponds to a physically later

time in the simulation. As the time increases in the simulation, the system reaches a point of equilibrium, whereby the spins in the system no longer flip as often as the overall energies become minimised. Mathematically, this is comparable to the 2D random walk, where since for each time step when the measurement is taken, the walk moves once in one of four directions. Due to low flip rate in this method, the autocorrelation between successive datasets are high, as is with a random walks method, only a single change per step.

Since the oversampling method by *Samarakoon et al.* tended to a decay exponent of $\beta = 1.95$, rather than the slightly higher value for the random walks, we hypothesise this to be due to random walks having no memory of their past movements, whereas the spins in spin ices do have some memory due to the energy of certain vertices being greater than others. An unconstrained random walk in 2D can move in one of four directions at each time step with equal probability, whereas in spin ices, there are varying probabilities of vertices, therefore not every spin can be flipped. This idea of memory directly changes the autocorrelation function for both, since the spin ice does not necessarily change its overall configuration at each time step. Overall, this changes the power spectral density, where we hypothesise that this causes the decay exponent to become $\beta < 2$ as it moves away from random Brownian noise to pink noise.

3.2 Future Work

As demonstrated, a completely unconstrained random walk method has a decay exponent tending to $\beta = 2$, therefore we recommend that there should be further investigation as to whether non-Markovian systems with memory will reduce the decay exponent from 2. Non-Markovian systems are those which contain an element of memory in their evolution, such that previous events affect the memory of future events [42]. One method to achieve this is through constrained random walks, this is where memory is applied to the system, so that for the random walker there are inhomogeneous probabilities for the direction of the walk at each step. This is to emulate how a spin has

certain probabilities of the flip occurring, depending on the energy cost, and if positive, whether the Boltzmann probability is greater than a fraction.

For example, a spin ice site of 3-in 1-out has four possible spins to be flipped. Going back to the original ground state of 2-in 2-out is always allowed by flipping the in spin. Similarly, the other two in spins can also be flipped, giving a 2-in 2-out ground state. However, flipping the out spin is forbidden here. This forms the constraints for the random walk method, where memory is incorporated by imposing two rules. If the new direction takes the random walker to the previous location, this is allowed, but otherwise the other three direction are accepted with $2/3$ probability.

If this method produces a power spectral density with a decay exponent $\beta < 2$, this allows us to characterise that completely random motion does indeed give Brownian noise with $\beta = 2$, but random motion with memory affecting the probability of occurrence will reduce the decay exponent. Furthermore, this will explain why *Samarakoon et al.* found decay exponent $\beta \approx 1.95$, since the spin ice system has memory.

We carried out some very initial simulations of unconstrained and constrained random walks with spin ice like memory which has shown the decay constant does not vary with memory introduced into the system, though more thorough investigations are needed.

4 Conclusion

This project undertook the task of characterising the power spectral density of a 2D artificial spin ice and finding the decay exponent as a function of temperature, with the express intention of comparing methods by *F. K. K. Kirschner et al.* [1] and *A. M. Samarakoon et al.* [2] to conclusively pronounce which method is correct.

The power spectral density is a very powerful tool and of great importance to the research of spin ice materials. 3D bulk spin ice materials begin to show ordering at very low temperatures, with the spin ice regime ranging between 0.6 K to 2 K where there are many magnetic monopole excitations.

Below this temperature, the spin ice reaches a zero magnetic monopole regime after it has equilibrated [43]. Ideally, a single monopole would be created in the spin ice and the resulting magnetic flux would be measured to prove its existence, though currently, this seems unfeasible. Therefore, one of the only current methods to characterise spin ices is through power spectral density calculations of the measurements due to the noise arising from the motion of many monopoles and comparing the decay exponent against variables such as applied magnetic field or temperature.

Furthermore, working with large numbers of magnetic monopoles may have more applications in the future, in areas such as magnetricity [20]. This is the use of magnetic monopoles instead of electrons as an analogue to electricity and thereby creating a magnetic current which may have applications in computing. These reasons mean it is vital to formulate the correct methods for finding the correct form of the decay exponent from the power spectral density.

Considering the methods from *F. K. K. Kirschner et al.*, measurements of the magnetisations were taken once per Monte Carlo step, obtaining decay exponents centring around $\beta \approx 0.95$ for a range of temperatures between $T \in [0.6, 1.1] K$ and corresponding applied field $\mathbf{B} \in [1.92k_b, 3.52k_b]$. This decay exponent is comparable to pink noise based on its power spectral density, which is in agreement with measurements undertaken by *F. K. K. Kirschner et al.* for bulk spin ice materials when the magnetic flux is measured in a SQUID device.

Using methods proposed by *A. M. Samarakoon et al.* and taking measurements of magnetisation per spin flip attempt for the same temperature and applied field region, two decay exponents are produced for two frequency regions, as seen in Figure 6. Firstly, considering the frequency region greater than the Nyquist frequency up to before the plateau, an average decay exponent of $\beta \approx 1.97$ was found. We argue that this is the frequency region which *A. M. Samarakoon et al.* fit the decay exponents over and that this is incorrect, since by measuring once per attempted flip, the Nyquist frequency actually becomes smaller by a factor of N . Accommodating for this fact, the true Nyquist frequency is identified and the corresponding true decay expo-

nents are extracted from the frequency region from the initial plateau at low frequencies to the true Nyquist frequency.

The true extracted decay exponents from the latter method are shown to agree with the decay exponents from the former method within their respective standard deviation, indicating the correct rate to sample is once per Monte Carlo step and by increasing this rate, the Nyquist frequency decreases proportionally leading to oversampling. Both methods of measuring once per Monte Carlo step produces decay exponents of $\beta \approx 0.95$, showing little in terms of trends as temperature is varied, indicating it is independent of temperature in this range.

For frequencies greater than the Nyquist frequency, the data will tend towards a plateau with gradient of zero, so that the data can be mirrored and aliased due to folding in the Fourier transform. We propose that this is the reason why *A. M. Samarakoon et al.* calculated $\beta \approx 1.95$ for the range of temperatures. Again, within standard deviation errors, the decay exponent found from Figure 6 of the region past the true Nyquist frequency to the plateau agree with the values cited in *A. M. Samarakoon et al.* [2] for the entire temperature region. This suggests that they use the incorrect frequency region to fit the decay exponent and that this region is not indicative of the characteristics of the spin ice material.

The decay exponent of $\beta = 2$ is generally known as Brownian noise, this is to indicate that this decay exponent is indicative of purely random motion which is not true for the motion of monopoles in spin ices, as is known to be a non-Markovian process. This due to the memory of which vertices are allowed after a certain flip due to the system's need to minimise energy. This notion is further emphasised through an unconstrained 2D random walk with decay exponent $\beta = 1.997 \pm 0.012$, which is a completely random (or Markovian) process. This further stipulates that this method measures past the true Nyquist frequency of the system in equilibrium, where there is simply random isolated cases of monopole movement which does not characterise the true monopole plasma region of the spin ice.

5 Acknowledgements

I would like to thank my supervisor Dr. F. Flicker for regular meetings and guidance with the project. Additionally, I would like to thank J. Colclough and S. Singh for discussions and insightful questions. Finally, I would like to thank Supercomputing Wales for access to the Hawk Cluster to run my simulations.

References

- [1] F. K. K. Kirschner, F. Flicker, A. Yacoby, N. Y. Yao, and S. J. Blundell. Proposal for the detection of magnetic monopoles in spin ice via nanoscale magnetometry. *Phys. Rev. B*, 97:140402, (2018).
- [2] A. M. Samarakoon, S. A. Grigera, D. A. Tennant, A. Kirste, B. Klemke, P. Strehlow, M. Meissner, J. N. Hallén, L. Jaubert, C. Castelnovo, and R. Moessner. Anomalous magnetic noise in an imperfectly flat landscape in the topological magnet $Dy_2Ti_2O_7$. *Proceedings of the National Academy of Sciences*, 119(5), (2022).
- [3] L. Jaubert, J. Chalker, P. Holdsworth, and R. Moessner. The kasteleyn transition in three dimensions: Spin ice in a [100] field. *Journal of Physics Conference Series*, 145, (2009).
- [4] M. Goryca, X. Zhang, J. Li, A. L. Balk, J. D. Watts, C. Leighton, C. Nisoli, P. Schiffer, and S. A. Crooker. Field-induced magnetic monopole plasma in artificial spin ice. *Phys. Rev. X*, 11:011042, (2021).
- [5] L. Pauling. The structure and entropy of ice and of other crystals with some randomness of atomic arrangement. *J. Am. Chem. Soc.*, 57(12):2680–2684, (1935).
- [6] S. T. Bramwell and M. J. Harris. The history of spin ice. *Journal of Physics: Condensed Matter*, 32(37):374010, (2020).

- [7] G. C. Lau, R. S. Freitas, B. G. Ueland, B. D. Muegge, E. L. Duncan, P. Schiffer, and R. J. Cava. Zero-point entropy in stuffed spin-ice. *Nature Physics*, 2(4):249–253, (2006).
- [8] P. A. M. Dirac. Quantised singularities in the electromagnetic field,. *Proc. Roy. Soc. Lond. A*, 133(821):60–72, (1931).
- [9] C. Castelnovo, R. Moessner, and S. L. Sondhi. Magnetic monopoles in spin ice. *Nature*, 451(7174):42–45, (2008).
- [10] D. J. P. Morris, D. A. Tennant, S. A. Grigera, B. Klemke, C. Castelnovo, R. Moessner, C. Czternasty, M. Meissner, K. C. Rule, J.-U. Hoffmann, K. Kiefer, S. Gerischer, D. Slobinsky, and R. S. Perry. Dirac strings and magnetic monopoles in the spin ice $\text{dy}_2\text{ti}_2\text{o}_7$. *Science*, 326(5951):411–414, (2009).
- [11] P. Stoica, L. Moses, and Randolph. *Spectral analysis of signals*. Pearson/Prentice Hall, Upper Saddle River, N.J., (2005).
- [12] J. F. Sadoc and R. Mosseri. *Geometrical Frustration*. Collection Alea-Saclay: Monographs and Texts in Statistical Physics. Cambridge University Press, (1999).
- [13] J. Snyder, J. Slusky, R. Cava, and P. Schiffer. How ‘spin ice’ freezes. *Nature*, 413:48–51, (2001).
- [14] L. Balents. Spin liquids in frustrated magnets. *Nature*, 464(7286):199–208, (2010).
- [15] A. P. Ramirez. Strongly geometrically frustrated magnets. *Annual Review of Materials Science*, 24(1):453–480, (1994).
- [16] R. F. Wang, C. Nisoli, R. S. Freitas, J. Li, W. McConville, B. J. Cooley, M. S. Lund, N. Samarth, C. Leighton, V. H. Crespi, and P. Schiffer. Artificial ‘spin ice’ in a geometrically frustrated lattice of nanoscale ferromagnetic islands. *Nature*, 439:303–306, (2006).

- [17] D. Levis. *Two-dimensional Spin Ice and the Sixteen-Vertex Model*. PhD thesis, Universite Pierre et Marie Curie - Paris VI, (2012).
- [18] L. F. Cugliandolo. Artificial Spin-Ice and vertex models. *Journal of Statistical Physics*, 167(3):499–514, (2017).
- [19] L. Foini, D. Levis, M. Tarzia, and L. F Cugliandolo. Static properties of 2d spin-ice as a sixteen-vertex model. *Journal of Statistical Mechanics: Theory and Experiment*, (2013)(02):02026, (2013).
- [20] C. Castelnovo. Coulomb physics in spin ice: From magnetic monopoles to magnetic currents. *ChemPhysChem*, 11(3):557–559, (2010).
- [21] T. Sergios. Chapter 2 - probability and stochastic processes. In S. Theodoridis, editor, *Machine Learning (Second Edition)*, pages (19–65. Academic Press, 2nd edition edition, (2020).
- [22] A. V. Klyuev, M. I. Ryzhkin, A. V. Yakimov, and B. Spagnolo. Memory effect and generation-recombination noise of magnetic monopoles in spin ice. *Journal of Statistical Mechanics: Theory and Experiment*, 20(9):094005, (2019).
- [23] C. Nisoli. The color of magnetic monopole noise. *Europhysics Letters*, 135(5):57002, (2021).
- [24] R. Dusad, F. K. K. Kirschner, J. C. Hoke, B. R. Roberts, A. Eyal, F. Flicker, G. M. Luke, S. J. Blundell, and J. C. Séamus Davis. Magnetic monopole noise. *Nature*, 571(7764):234–239, (2019).
- [25] H. Pishro-Nik. *Introduction to Probability, Statistics and Random Processes*, page 771–774. Kappa Research LLC, 1st edition, (2014).
- [26] W. Gerstner, W. M. Kistler, R. Naud, and L. Paninski. *Neuronal Dynamics*, page 168–169. Cambridge University Press, 1st edition, (2014).
- [27] W. Franklin A. B. Downey. *Think DSP: Digital Signal Processing in Python*, pages 51–62. Green Tea Press, (2012).

- [28] B. Huitema and S. Laraway. *Autocorrelation*. SAGE Publications, (2006).
- [29] J. Rau and M. Gingras. Spin slush in an extended spin ice model. *Nature Communications*, 7, (2016).
- [30] A. Lapidoth. *Operational Power Spectral Density*, page 257–294. Cambridge University Press, 2nd edition, (2017).
- [31] S. V. Vaseghi. *Power Spectrum and Correlation*, chapter 9, pages 263–296. John Wiley and Sons, Ltd, 4th edition, (2000).
- [32] A. P. Hatzes. Frequency analysis of time series data. In *The Doppler Method for the Detection of Exoplanets*, 2514-3433, pages 7–1 to 7–36. IOP Publishing, (2019).
- [33] R. Oshana. Dsp software development techniques for embedded and real-time systems. *DSP Software Development Techniques for Embedded and Real-Time Systems*, pages 19–27, (2006).
- [34] M. H. White. A monte carlo study on methods for handling class imbalance. (2017).
- [35] D. P. Kroese R. Y. Rubinstein. *Simulation and the Monte Carlo method*, pages 1–46. John Wiley and Sons, inc, (2017).
- [36] C. Nisoli, J. Li, X. Ke, D. Garand, P. Schiffer, and V. H. Crespi. Effective temperature in an interacting vertex system: Theory and experiment on artificial spin ice. *Phys. Rev. Lett.*, 105:047205, (2010).
- [37] J. Amaral, J. Goncalves, and V. Amaral. Thermodynamics of the 2-d ising model from a random path sampling method. *IEEE Transactions on Magnetics*, 50:1002204, (2014).
- [38] R. Harms and A. Roebroeck. Robust and fast markov chain monte carlo sampling of diffusion mri microstructure models. *Frontiers in Neuroinformatics*, 12:97, (2018).

- [39] E. Robinson and D. Clark. Sampling and the nyquist frequency. *The Leading Edge*, 10(3):51–53, (1991).
- [40] W. L. Gans and N. S. Nahman. Continuous and discrete fourier transforms of steplike waveforms. *IEEE Transactions on Instrumentation and Measurement*, IM-31(2):97–101, (1982).
- [41] G. D. Bergland. A guided tour of the fast fourier transform. *IEEE Spectrum*, 6(7):41–52, (1969).
- [42] G. A. L. White, C. D. Hill, F. A. Pollock, L. C. L. Hollenberg, and K. Modi. Demonstration of non-markovian process characterisation and control on a quantum processor. *Nature Communications*, 11(1), (2020).
- [43] L. D. C. Jaubert and P. C. W. Holdsworth. Magnetic monopole dynamics in spin ice. *Journal of Physics: Condensed Matter*, 23(16):164222, (2011).